THE JOURNAL OF PHYSICAL CHEMISTRY A

Article

pubs.acs.org/JPCA

# Solubilities and Glass Formation in Aqueous Solutions of the Sodium Salts of Malonic Acid With and Without Ammonium Sulfate

Jared A. Kissinger,[†] Lukas G. Buttke,[†] Anastasiya I. Vinokur,[‡] Ilia A. Guzei,[‡] and Keith D. Beyer*[,†]

[†]Department of Chemistry and Biochemistry, University of Wisconsin-La Crosse, La Crosse, Wisconsin 54601, United States

[‡]Chemistry Department, University of Wisconsin-Madison, Madison, Wisconsin 53706, United States

Supporting Information

**ABSTRACT:** The solubility of sodium hydrogen malonate and sodium malonate in water both with and without ammonium sulfate present has been studied using differential scanning calorimetry and infrared spectroscopy. The crystals that form from sodium hydrogen malonate/water solutions were determined to be sodium hydrogen malonate monohydrate by single-crystal X-ray diffractometry. The crystals formed in sodium malonate/water solutions were determined to be sodium malonate monohydrate, a compound whose structure had not been previously known. When ammonium sulfate is added to these respective aqueous systems, the precipitation solids contain sodium sulfate decahydrate under low to moderate ammonium concentrations and lecontite ($NaNH_4SO_4{\cdot}2H_2O$) under high ammonium concentrations, which can be found under dry atmospheric conditions. Thus, it appears the presence of malonate and hydrogen malonate ions does not significantly affect the precipitation of inorganic salts in these systems. The glass transition temperatures of all solutions were also determined, and it was observed that the addition of ammonium sulfate slightly lowers the glass transition temperature in these solutions.

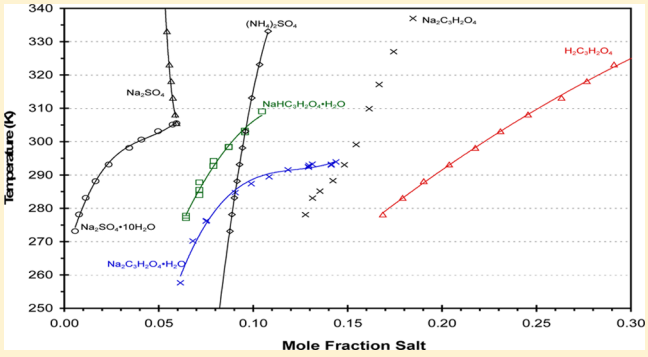


## INTRODUCTION

Field measurements of aerosols in the free and upper troposphere (UT) have shown that the major chemical components are sulfates, nitrates, ammonium, organic species, and mineral dust.[1,2] Among the organic components, dicarboxylic acids are present in aerosols in a range of environments especially for aerosols that have undergone chemical aging.[3] Dicarboxylic acids are found in primary organic aerosols as well as secondary organic aerosols.[4] Aerosols also commonly contain mineral dust whose components can be leached to the aqueous phase through chemical aging, especially under acidic conditions.[5,6] The metals at the surface or reacted to the aqueous phase of mineral dust particles can enhance the chemistry that occurs in the aqueous phase.[5,7] Field studies have shown an abundance of aerosols with organics and metals/metal salts from sea spray (Na, Mg),[3,8−10] biomass burning (K),[11,12] and mineral dusts/meteoritic material (Na, K, Ca, Fe).[1,13−16] Field and lab studies have shown that metal ions can displace hydrogen ions from organic acids to form carboxylate salts in atmospheric aerosols.[8,10,17,18] For example, for a particle with dissolved NaCl and malonic acid that experienced UT temperatures and/or dry conditions, we would have

$$n\mathrm{NaCl(aq)} + \mathrm{H_2C_3H_2O_4(aq)} \rightarrow \mathrm{Na}_n\mathrm{H}_{2-n}\mathrm{C_3H_2O_4(s)} + n\mathrm{HCl(aq, g)} \quad (1)$$

where $n$ = 1 or 2. Studies have shown that the HCl product is highly volatile, leaving behind the organic salt in the particle.[10,17] As the particle experiences cold/dry conditions in the atmosphere, the sodium malonate salt could precipitate or contribute to glass formation of the aqueous phase of the aerosol.[18] However, there is very limited information in the literature regarding the solubilities, glass formation properties, or other thermodynamic data at free and UT temperatures for carboxylate salts and are not taken into account in atmospheric aerosol composition models.[19,20] In addition, nothing is known about how the presence of ammonium sulfate could affect solubility or other thermodynamic properties. Thus, there is clearly a need for solubility data as a function of temperature for metal-carboxylate salts in water and in the presence of ammonium sulfate.

It has also been shown that aerosols containing inorganic and organic components of sufficiently high molecular weight can form glasses rather than crystallize at temperatures relevant for the troposphere.[21,22] Additionally, laboratory studies have shown that some glasses may be efficient at ice nucleation.[23] However, there is a limited amount of experimental data on inorganic/organic systems representative of free and upper tropospheric aerosols with respect to glass transition temper-

**Received:** March 14, 2016
**Revised:** April 19, 2016
**Published:** May 12, 2016





DOI: 10.1021/acs.jpca.6b02656
J. Phys. Chem. A 2016, 120, 3827−3834

atures and whether glass formation in these systems is a prerequisite for ice formation (see review of Koop et al.[22]).

## EXPERIMENTAL SECTION

**Sample Preparation.** Solutions to be studied in DSC and FTIR experiments were made by mixing malonic acid (99%, Acros Organics), ammonium sulfate (99+%, Sigma-Aldrich), and sodium hydroxide (beads, Fisher) with deionized water. For X-ray crystallography experiments, a single crystal was extracted from a saturated solution.

**Differential Scanning Calorimetry.** Thermal data were obtained with several Mettler Toledo DSC instruments: 822e and DSC1 with liquid nitrogen cooling and 822e and DSC1 cooled via an intra cooler. The 822e instruments utilized an HSS7 sensor, while the DSC1 instruments utilize an FRS5 sensor. High-purity grade nitrogen was used as a purge gas with a flow rate of 50 mL per minute. The temperature reproducibility of these instruments is better than ±0.05 K. Our accuracy is estimated to be ±0.9 K with a probability of 0.94 based on a four-point temperature calibration[24] using indium, HPLC grade water, anhydrous, high purity (99%+) octane, and anhydrous, high purity heptane (99%+) from Aldrich, the latter three stored under nitrogen. The enthalpy/heat capacity measurement of each DSC was also calibrated using the same substances and the known enthalpy of fusion for each substance yielding an accuracy of ±3% with a probability of 0.92.

Samples were contained in 40 μL aluminum pans with crimped lids to create a seal and typically had a mass of approximately 15−25 mg. In some instances to increase probability of crystallization larger samples sizes were used (about 70 mg) in platinum pans with lids that were not sealed. A typical sample was cooled to 183 at 10 K per minute, held at that temperature for 5 min, and then warmed at a rate of 1 K per minute to a temperature at least 5 K above the predicted dissolution point.

**Infrared Spectra.** The sample cell used for infrared spectra of liquid samples is similar to that described in previous literature.[25] A small drop of solution was placed between two ZnSe windows, which were held in the center of an aluminum block by a threaded metal ring. Sample volumes were approximately 2 μL. On each side of the aluminum block, a Pyrex cell was purged with dry nitrogen gas. KBr windows were placed on the end of each cell, sealed with o-rings and held in place by metal clamps. The sample was cooled by pouring liquid nitrogen into a circular aluminum cup attached to the top of the main cell. The cell block was warmed by resistive heaters connected to a temperature controller. Temperature was measured by a copper/constantan thermocouple placed at the edge of the ZnSe windows and connected to the temperature controller. The temperature of the cell was calibrated using HPLC grade water and high purity organic solvents (Aldrich), decane, octane and acetic anhydride of which the melting points are 243.5, 216.4, and 200.2 K, respectively.[26] The IR cell temperatures are known on average to within ±1.3 K, that is, a temperature we measured in the IR cell of a specific transition is within 1.3 K of the transition temperature we measure (of the same transition) using the DSC. For solid samples, a Pike Technologies Miracle ATR accessory was used at room temperature (approximately 293 K).

Spectra were obtained with a Bruker Tensor 37 FTIR with a DTGS detector at 4 $cm^{-1}$ resolution. Each spectrum was the average of 8 scans. Before spectra were taken of a sample, a background scan was obtained from a dry, purged sample cell (or an empty ATR cell for the solid samples). Liquid samples were cooled until the sample completely froze or to 200 K (which ever was a higher temperature) at 3 K per minute and then allowed to warm to room temperature without resistive heating, typically this was 1 K/min or less. If the final target temperature was above room temperature, then resistive heating was applied to increase temperature at about 1 K/min.

**X-ray Crystallography.** The crystal structure of $Na_2C_3H_2O_4{\cdot}H_2O$ (Figure 1) was solved in a routine fashion

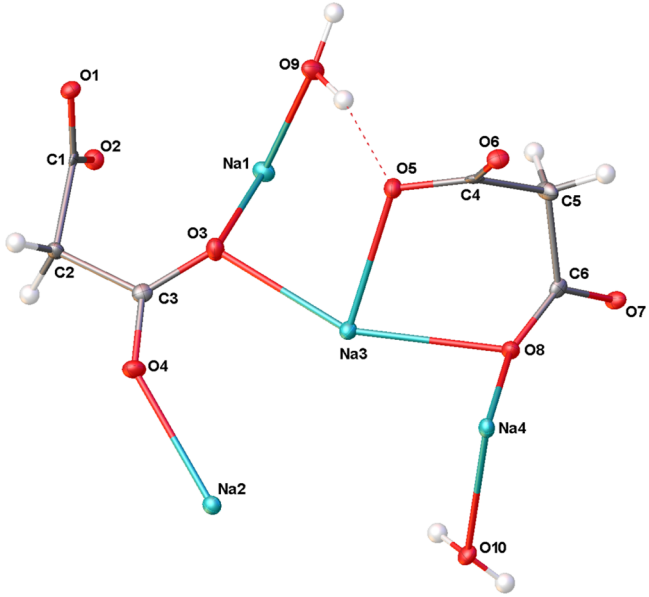


**Figure 1.** A molecular drawing of $Na_2C_3H_2O_4{\cdot}H_2O$ shown with 50% probability ellipsoids.

(see Supporting Information). The asymmetric unit contains four symmetry-independent Na cations, two malonates, and two aqua ligands. The cations, ions, and aqua ligands are connected to form a three-dimensional framework. Atoms Na1 and N3 are six-coordinate, whereas Na2 and Na4 are five-coordinate.

Crystal Data for $(Na_2C_3H_2O_4{\cdot}H_2O)_2$ (M = 166.04 g/mol): monoclinic, space group $P2_1/c$ (no. 14), $a$ = 10.4604(7) Å, $b$ = 15.2727(11) Å, $c$ = 7.3353(5) Å, $\beta$ = 104.354(3)°, $V$ = 1135.30(14) $Å^3$, $Z$ = 8, $T$ = 99.98 K, $\mu$(CuK$\alpha$) = 2.870 $mm^{-1}$, $D_{calc}$ = 1.943 g/$cm^3$, 16184 reflections measured (8.726° ≤ 2Θ ≤ 146.73°), 2246 unique ($R_{int}$ = 0.0221, $R_{sigma}$ = 0.0111) which were used in all calculations. The final $R_1$ was 0.0242 ($I > 2\sigma(I)$) and $wR_2$ was 0.0649 (all data).

## RESULTS

**$NaHC_3H_2O_4$.** We made aqueous solutions of various concentrations with a 1:1 mol ratio of $NaOH{:}H_2C_3H_2O_4$. The concentrations studied covered the range of 0−45 wt % $NaHC_3H_2O_4$. There appears to be no information on this system in water in the literature. DSC and IR experiments were performed on the solutions to determine both solubility and glass transition temperatures. This data is compiled in Figure 2, which constitutes a partial phase diagram of $NaHC_3H_2O_4/H_2O$. It is seen that the melting points at $[NaHC_3H_2O_4] < 26.2$ wt % represent the depressed melting points of ice, and the solid/liquid equilibrium points at higher concentrations represent the solubility of the compound formed in this solution. We were


DOI: 10.1021/acs.jpca.6b02656
J. Phys. Chem. A 2016, 120, 3827−3834

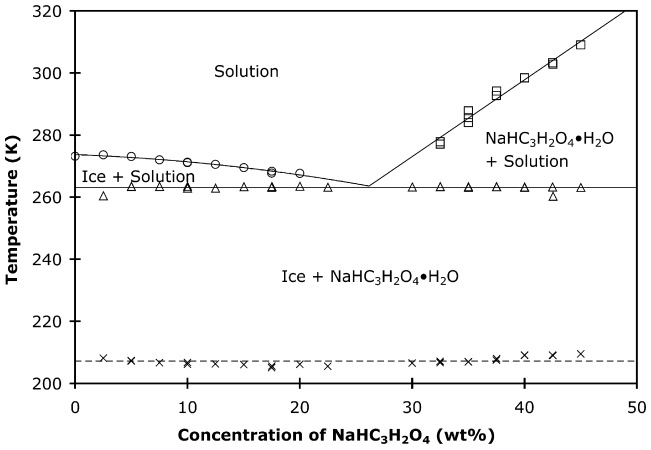


**Figure 2.** Partial phase diagram of the $NaHC_3H_2O_4/H_2O$ system. Circles, ice melting; squares, solubility of $NaHC_3H_2O_4{\cdot}H_2O$; triangles, eutectic melting; crosses, glass transition temperature ($T_g'$ see text for definition). Solid lines are fits to the data as given in the text. Dashed line represents the average glass transition temperature of 207 ± 1 K.

able to easily make saturated solutions of this compound, and a single crystal from a saturated solution was used for X-ray crystallographic analysis. The analysis determined that the salt present is $NaHC_3H_2O_4{\cdot}H_2O$ (sodium hydrogen malonate monohydrate) by a match of the unit cell data with this compound in the Cambridge Crystallographic Database.[27] We acquired an IR spectrum of crystals removed from a saturated solution that were subsequently dried before analysis. The IR spectrum for $NaHC_3H_2O_4{\cdot}H_2O$ is given in Figure 3. The ice

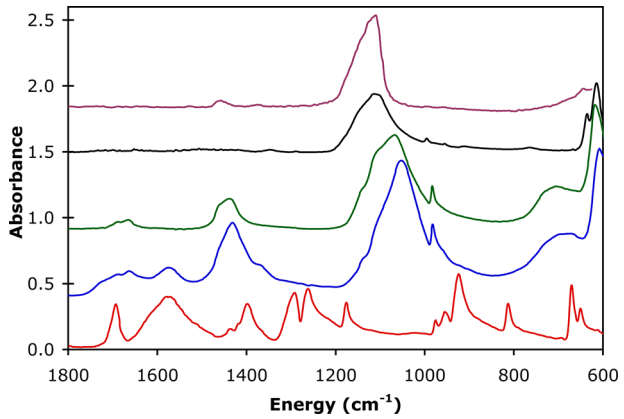


**Figure 3.** Infrared spectra of several samples taken with an ATR accessory. Red line, $NaHC_3H_2O_4{\cdot}H_2O$; blue line, solids from 30/25% $(NH_4)_2SO_4/NaHC_3H_2O_4$; green line, solid from 20/25% $(NH_4)_2SO_4/NaHC_3H_2O_4$ that is a nearly identical match with the spectrum of lecontite as given by Kloprogge et al.;[35] black line, solid from 10/30% $(NH_4)_2SO_4/NaHC_3H_2O_4$; magenta line, digitized NIST spectrum for $Na_2SO_4$.[36] Spectra are offset for clarity and multiplied to normalize the sulfate bands by the following (offset/multiplier): red (+0.08/8), blue (+0.35/1.8), green (+0.9/8), black (+1.5/5), magenta (+1.8/1).

melting and $NaHC_3H_2O_4{\cdot}H_2O$ solubility temperatures were fit to the following equation

$$T = A_2x^2 + A_1x + A_0 \quad (2)$$

where $x$ is the wt % of $NaHC_3H_2O_4$ in solution, $T$ is temperature in Kelvin, and $A_i$ are the polynomial coefficients as given in Table 1. By solving the equations for the ice melting

**Table 1. Polynomial Coefficients for Fit to Solubility Data According to Equation 2**

| entity | $A_2$ | $A_1$ | $A_0$ |
|---|---|---|---|
| | $NaHC_3H_2O_4/H_2O$ | | |
| ice | −0.009613 | −0.1349 | 273.7 |
| $NaHC_3H_2O_4{\cdot}H_2O$ | | 2.476 | 198.7 |
| | $Na_2C_3H_2O_4/H_2O$ | | |
| ice | −0.01147 | −0.1929 | 273.5 |
| $Na_2C_3H_2O_4{\cdot}H_2O$ | −0.07686 | 8.531 | 56.34 |

and $NaHC_3H_2O_4$ dissolution, the ice/$NaHC_3H_2O_4$ eutectic was determined to be 26.2 wt % $NaHC_3H_2O_4$ with the average eutectic temperature from the DSC data equal to 263.1 ± 0.8 K.

We were also able to obtain the glass transition temperature (onset of the glass transition on heating following the recommendation of Angell[28] and Dette and Koop[29]) for each solution studied, and these data are plotted in Figure 2. It is seen that the values of the glass transition are nearly constant as a function of sample concentration. This is because in each case there was partial crystallization of the liquid (most likely ice) upon cooling, thus the concentration of the remaining liquid at the glass transition was the same for each sample. Following previous practice,[30,31] we utilize the symbol $T_g'$ to indicate a glass transition where part of the sample crystallized and part is still solution, which undergoes a glass transition in the cooling segment and reverses in the warming segment. The average value of the measured $T_g'$ is 207 ± 1 K. The raw DSC data for this system is given in Table S1 in the Supporting Information.

**$NaHC_3H_2O_4/(NH_4)_2SO_4$.** We explored the effect of ammonium sulfate on solutions of sodium hydrogen malonate. Solutions were made adding NaOH and $H_2C_3H_2O_4$ in a 1:1 ratio to aqueous solutions, which were also 10, 20, or 30 wt % $(NH_4)_2SO_4$. Multiple crystallization and melting/dissolution transitions were observed in these samples as well as glass transitions in DSC and IR experiments. In IR experiments, the entire liquid phase tended to crystallize simultaneously. Because of the complexity of these solutions and overlapping IR absorption bands, it was not possible to uniquely identify all phases present at any given temperature from the IR and DSC data alone. However, it is generally clear in an IR spectrum when ice melts, and a consistent value for the ternary eutectic was observed in DSC experiments and confirmed with IR experiments. We have correlated the IR data with the DSC data for ice melting and report this raw data in Table S2 in the Supporting Information. The average value of the ternary eutectic was found to be 249 ± 4 K from DSC experiments.

We focused our main attention on the last crystalline phase to be present on warming before the sample converted to a completely liquid solution (highest temperature endothermic transition in the DSC data). The solubility data is presented in Figure 4 with the raw data given in Table S2 in the Supporting Information. For a given temperature, the presence of ammonium sulfate significantly reduced the concentration of $NaHC_3H_2O_4$ at which a solid is in equilibrium with solution. Only a weak dependence is seen on the amount of $(NH_4)_2SO_4$ present. With the mixture of ions present in solution ($Na^+$, $NH_4^+$, $HC_3H_2O_4^-$, and $SO_4^{2-}$) we considered the possibility that a new compound was precipitating from solution that is less soluble than either $(NH_4)_2SO_4$ or $NaHC_3H_2O_4$. At the highest total salt concentrations ($(NH_4)_2SO_4$ + $NaHC_3H_2O_4$), we observed crystals form from solution at room temperature.


DOI: 10.1021/acs.jpca.6b02656
J. Phys. Chem. A 2016, 120, 3827−3834

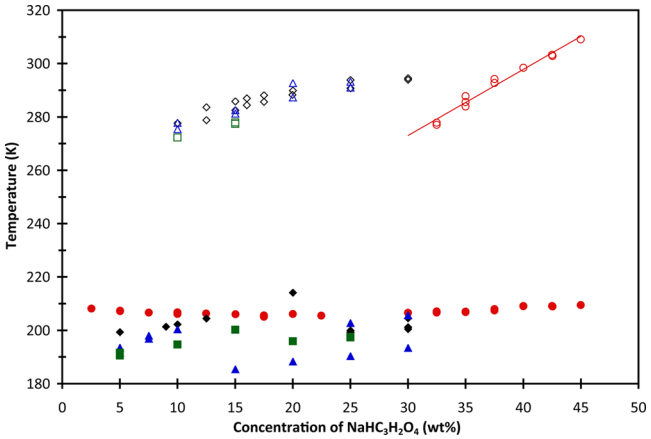


**Figure 4.** Solubility for solutions of $NaHC_3H_2O_4/H_2O$ with $(NH_4)_2SO_4$ present. Open red circles, $NaHC_3H_2O_4$ with no $(NH_4)_2SO_4$; open black diamonds, $NaHC_3H_2O_4$ with 10 wt % $(NH_4)_2SO_4$ present; open blue triangles, $NaHC_3H_2O_4$ with 20 wt % $(NH_4)_2SO_4$ present; open green squares, $NaHC_3H_2O_4$ with 30 wt % $(NH_4)_2SO_4$ present. Glass transition temperatures ($T_g'$) as defined in the text are given as the following solid symbols at the lower temperatures in the figure: solid red circles, $NaHC_3H_2O_4$ with no $(NH_4)_2SO_4$; solid black diamonds, $NaHC_3H_2O_4$ with 10 wt % $(NH_4)_2SO_4$ present; solid blue triangles, $NaHC_3H_2O_4$ with 20 wt % $(NH_4)_2SO_4$ present; solid green squares, $NaHC_3H_2O_4$ with 30 wt % $(NH_4)_2SO_4$ present.

To determine the identity of these crystals, they were removed from a solution of 30/25 wt % $(NH_4)_2SO_4/NaHC_3H_2O_4$ at room temperature and analyzed for crystal structure with X-ray crystallography. The analysis determined that the salt present is $NaNH_4SO_4{\cdot}2H_2O$ (sodium ammonium sulfate dihydrate) by a match of the unit cell data with this compound in the Inorganic Crystal Structural Database (ICSD) entered by Arzt and Glazer.[32] This compound has been known for some time in mineralogy and has been found to be structurally equivalent to the mineral lecontite found in nature.[33] It has also been identified as the most stable phase at high $(NH_4)_2SO_4$ and moderate $Na_2SO_4$ concentrations in the $(NH_4)_2SO_4/Na_2SO_4/H_2O$ system.[34] We also removed crystals from this solution and air-dried them at room temperature for several days for IR analysis using an ATR accessory. The resulting spectrum is given in Figure 3 and is found to be composed of features of lecontite (as reported by Kloprogge et al.[35] for $NaNH_4SO_4{\cdot}2H_2O$) and $NaHC_3H_2O_4{\cdot}H_2O$, which is expected since this solid would crystallize as water evaporated from the sample.

To determine if solutions of other concentrations were also precipitating lecontite, we cooled several solutions of various concentrations in liquid nitrogen until the solution completely solidified. The samples were then placed in an ice bath at 273 K for 30 min. If crystals were observed to be present in the solution, they were removed and allowed to air dry at room temperature until the solids visually looked dry (typically 24 h). Samples of the crystals were then placed in an ATR accessory for IR analysis. No crystals were visible for some solutions either because all crystals had dissolved at 273 K or there were too few present to be visible, that is, 10/15, 20/20, and 30/10 wt % $(NH_4)_2SO_4/NaHC_3H_2O_4$. However, for other solutions crystals were recovered, that is, 10/30, 20/25, 30/15, 30/25 wt % $(NH_4)_2SO_4/NaHC_3H_2O_4$. For the 10/30 wt % $(NH_4)_2SO_4/NaHC_3H_2O_4$ solution, the crystalline phase was determined to be $Na_2SO_4$ with IR analysis (see Figure 3) by a match with the known IR spectrum of $Na_2SO_4$.[36] This result is not surprising since $Na_2SO_4$ is less soluble than either $(NH_4)_2SO_4$ or $NaHC_3H_2O_4$.[37] (We note that the dry atmospheric conditions of our lab favor the formation of $Na_2SO_4$ over $Na_2SO_4{\cdot}10H_2O$ whose equilibrium relative humidity (RH) at 298 K is 80.7%. At RH values below this the decahydrate will convert to the anhydrous sodium sulfate with the reverse being true at RH > 80.7 but less than 93.6% RH, which is the DRH of $Na_2SO_4{\cdot}10H_2O$.[38]) For solutions of other concentrations, the crystals formed were determined to be lecontite by a match with the IR spectrum as described above along with a small amount of $NaHC_3H_2O_4{\cdot}H_2O$ that formed from the drying solution that clung to the crystals we removed from the bulk solution. The crystals removed from one solution (20/25 wt % $(NH_4)_2SO_4/NaHC_3H_2O_4$) yielded an IR spectrum that appeared to be an exact match with that given by Kloprogge et al.[35] and we have shown this spectrum for reference in Figure 3. Thus, it appears that at high total salt concentrations ($[(NH_4)_2SO_4] + [NaHC_3H_2O_4] \geq 40$ wt %) lecontite is the least soluble solid in this system, whereas at lower total salt concentrations ($[(NH_4)_2SO_4] + [NaHC_3H_2O_4] \leq 40$ wt %) $Na_2SO_4$ (or $Na_2SO_4{\cdot}10H_2O$) is the least soluble solid in this system. This observation may be surprising in a system that has a large fraction of organic species present but it does mirror the $(NH_4)_2SO_4/Na_2SO_4/H_2O$ system in terms of the solubility of $Na_2SO_4/Na_2SO_4{\cdot}10H_2O$ and $NaNH_4SO_4{\cdot}2H_2O/Na_2SO_4{\cdot}10H_2O$ is less soluble at low ammonium sulfate concentrations over a wide range of $Na_2SO_4$ concentrations, while $NaNH_4SO_4{\cdot}2H_2O$ is less soluble at high $(NH_4)_2SO_4$ concentrations and low to moderate $Na_2SO_4$ concentrations. A plot of a portion of the $(NH_4)_2SO_4/Na_2SO_4/H_2O$ phase diagram from the data of Stephen et al.[34] is given in Figure S1 in the Supporting Information where this is visually represented. Therefore, it appears the concentrations of $Na^+$, $NH_4^+$, and $SO_4^{2-}$ in the $(NH_4)_2SO_4/NaHC_3H_2O_4/H_2O$ system are the determining factors in the precipitation of the least soluble solid, which is an inorganic species with no organic portion.

The glass transition temperatures as a function of $NaHC_3H_2O_4$ concentration are also plotted in Figure 4 and values are given in Table S2 in the Supporting Information. In all of these solutions, partial crystallization was observed on cooling, thus the glass transition temperatures ($T_g'$) are likely for solutions of a constant concentration. As stated above, the average $T_g'$ value equals 207 ± 1 K for the $NaHC_3H_2O_4$ binary system. Addition of $(NH_4)_2SO_4$ had only a slight effect in decreasing the value of $T_g'$. Also, as seen in Figure 4, no clear trend in the value of $T_g'$ is seen as a function of the concentration of $(NH_4)_2SO_4$. Separate crystallization events were clear in DSC experiments, however in IR experiments we always observed cocrystallization of the various phases. However, if lecontite is crystallizing on cooling (as the least soluble solid for most samples), then a very weak effect on $T_g'$ would be expected as most sulfate, sodium, and ammonium ions would be in the solid phase, which does not effect $T_g'$.

**$Na_2C_3H_2O_4$.** We made solutions of various concentrations with a 2:1 mol ratio of $NaOH/H_2C_3H_2O_4$. The concentrations studied covered the range of 0−58 wt % $Na_2C_3H_2O_4$. DSC and IR experiments were performed on the solutions to determine both solubility and glass transition temperatures. This data is compiled in Figure 5, which constitutes a partial phase diagram of $Na_2C_3H_2O_4/H_2O$. Raw data for this system is given in Table S3 in the Supporting Information. The solubility of $Na_2C_3H_2O_4$ has been investigated by Rozaini and Brimblecombe[39] and their


DOI: 10.1021/acs.jpca.6b02656
J. Phys. Chem. A 2016, 120, 3827−3834

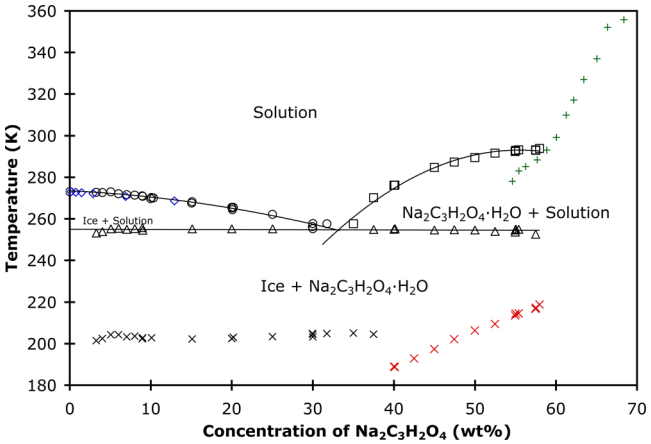


**Figure 5.** Partial phase diagram of $Na_2C_3H_2O_4/H_2O$. Symbols are black circles, ice melting; black squares solubility of $Na_2C_3H_2O_4·H_2O$; black triangles, eutectic melting; black crosses, glass transition temperature ($T_g'$) for solutions that partially crystallized on cooling; red crosses, $T_g$ for solutions that remained liquid to the glass transition; blue diamonds, ice melting data from Linke;[37] green pluses, $Na_2C_3H_2O_4$ solubility data from Rozaini and Brimblecombe.[39]

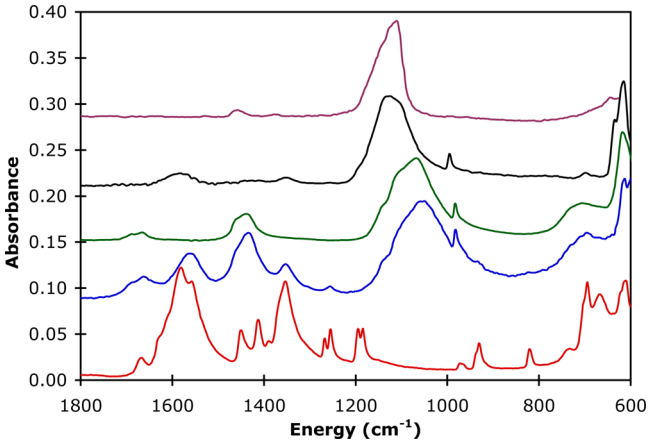


**Figure 6.** Infrared spectra of several samples taken with an ATR accessory. Red lines, $Na_2C_3H_2O_4·H_2O$; blue lines, solids from 30/20% $(NH_4)_2SO_4/Na_2C_3H_2O_4$; green lines, solid from 20/25% $(NH_4)_2SO_4/NaHC_3H_2O_4$ that is a nearly identical match with the spectrum of lecontite as given by Kloprogge et al.;[35] black lines, solid from 10/30% $(NH_4)_2SO_4/Na_2C_3H_2O_4$; magenta lines, digitized NIST spectrum for $Na_2SO_4$.[36] Spectra are offset for clarity and multiplied to normalize the sulfate bands by the following (offset/multiplier): red (+0.005/2), blue (+0.08/1), green (+0.15/1), black (+0.21/2.5), magenta (+0.28/0.15).

data are plotted in Figure 5. In their case, samples were made from crystals of the salt available commercially. Also, they determined solubility by dissolving the crystals completely and then cooling the solution, noting the temperature at which crystallization from solution occurred. We note that a caveat to this procedure is the possibility of supercooling of the solution, which would lead to lower observed solubility temperatures than true solid/liquid equilibrium. Data is also available[37] for the ice melting point depression in this system for concentrations up to 13 wt % $Na_2C_3H_2O_4$ and is plotted in Figure 5. Good agreement is seen between the literature ice melting points and our data. Our melting points at $[Na_2C_3H_2O_4]$ < 33.1 wt % represent the depressed melting points of ice, and the solid/liquid equilibrium points at higher concentrations represent the solubility of the compound formed in this solution. We were able to easily make saturated solutions of this compound, and a single crystal from a saturated solution was used for X-ray crystallographic analysis. The analysis determined that the salt present is $Na_2C_3H_2O_4·H_2O$, or sodium malonate monohydrate with a molecular drawing given in Figure 1. The structure of this compound has not previously been documented, and we discuss the structure solution and refinement in the Supporting Information. Thus, the solid/liquid equilibrium data for 33.1 < $[Na_2C_3H_2O_4]$ < 58 wt % represents the solubility as a function of temperature for $Na_2C_3H_2O_4·H_2O$. We also acquired an IR spectrum of crystals removed from a saturated solution and dried before analysis. The IR spectrum for these crystals, which we conclude to be $Na_2C_3H_2O_4·H_2O$ is given in Figure 6. The ice melting and $Na_2C_3H_2O_4·H_2O$ solubility temperatures were fit to eq 2 where $x$ is the wt % of $Na_2C_3H_2O_4$ in solution, $T$ is temperature in Kelvin, and $A_i$ are the polynomial coefficients as given in Table 1. By solving the equations for the ice melting and $Na_2C_3H_2O_4·H_2O$ dissolution, the ice/$Na_2C_3H_2O_4·H_2O$ eutectic was determined to be 33.1 wt % $Na_2C_3H_2O_4$ with the average eutectic temperature from the DSC data equal to 254.8 ± 0.8 K.

We also present the glass transition values for this system in Figure 5 with values given in Table S3 in the Supporting Information, where we observe nearly constant values up to 40 wt % $Na_2C_3H_2O_4$. At these concentrations, partial crystallization of the sample is seen on cooling and the average value of $T_g'$ is 203 ± 1 K, which is slightly lower than the value for $NaHC_3H_2O_4$. At $Na_2C_3H_2O_4$ concentrations of 40 wt % and higher, we observe an increasing value for the glass transition temperature as $Na_2C_3H_2O_4$ concentration increases. In these samples, we did not observe crystallization on cooling in DSC experiments; crystallization only occurred in the heating segment at temperatures above the glass transition, thus the entire sample is undergoing a glass transition for these concentrations, and thus we use the symbol $T_g$ for this glass transition. $T_g$ is predicted to change with solution concentration as has been shown for mixed inorganic/organic particles,[29] and our results are consistent with these predictions and observations.

**$Na_2C_3H_2O_4/(NH_4)_2SO_4$.** We then explored the effect of $(NH_4)_2SO_4$ on solubility and glass transitions in the $Na_2C_3H_2O_4/H_2O$ system. Solutions were made adding NaOH and $H_2C_3H_2O_4$ in a 2:1 ratio to water. Ammonium sulfate was then added to the solution. We studied solutions with 10, 20, or 30 wt % $(NH_4)_2SO_4$ and varying concentrations of $Na_2C_3H_2O_4$. There are many similarities between this system and the $NaHC_3H_2O_4/(NH_4)_2SO_4$ aqueous system described earlier. We again observed multiple crystallization and melting/dissolution transitions in these samples as well as glass transitions, but as in the $NaHC_3H_2O_4/(NH_4)_2SO_4$ aqueous system we focused our attention on the last crystalline phase to be present on warming before the sample converted to a completely liquid solution (highest temperature endothermic transition in the DSC data). The solubility data is presented in Figure 7, and the raw data is listed in Table S4 in the Supporting Information. Correlating the IR and DSC experiments, we were able to determine the temperature of ice melting in the solution as it warmed, and these values are given in Table S4. The average value of the ternary eutectic from DSC experiments is 231.9 ± 0.5 K, which is significantly lower than that found in the $(NH_4)_2SO_4/NaHC_3H_2O_4/H_2O$ system. With respect to solubility, it is seen that the addition of


DOI: 10.1021/acs.jpca.6b02656
J. Phys. Chem. A 2016, 120, 3827−3834

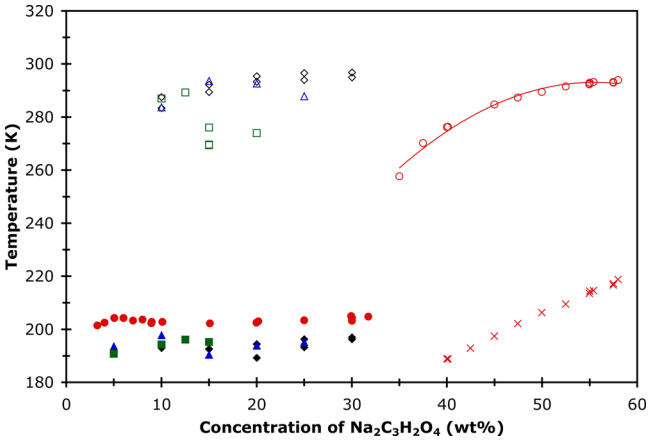


**Figure 7.** Solubility for solutions of $Na_2C_3H_2O_4/H_2O$ with $(NH_4)_2SO_4$ present. Open red circles, $Na_2C_3H_2O_4$ with no $(NH_4)_2SO_4$; open black diamonds, $Na_2C_3H_2O_4$ with 10 wt % $(NH_4)_2SO_4$ present; open blue triangles, $Na_2C_3H_2O_4$ with 20 wt % $(NH_4)_2SO_4$ present; open green squares, $Na_2C_3H_2O_4$ with 30 wt % $(NH_4)_2SO_4$ present. Glass transition temperatures ($T_g'$) as defined in the text are given as solid symbols at the lower temperatures in the figure: solid red circles, $Na_2C_3H_2O_4$ with no $(NH_4)_2SO_4$; solid black diamonds, $Na_2C_3H_2O_4$with 10 wt % $(NH_4)_2SO_4$ present; solid blue triangles, $Na_2C_3H_2O_4$with 20 wt % $(NH_4)_2SO_4$ present; solid green squares, $Na_2C_3H_2O_4$ with 30 wt % $(NH_4)_2SO_4$ present. Red crosses represent the glass transition temperature ($T_g$) where the sample remained liquid up to the glass transition (no crystallization) for $Na_2C_3H_2O_4/H_2O$ binary solutions.

$(NH_4)_2SO_4$ to $Na_2C_3H_2O_4/H_2O$ solutions significantly decreases the solubility of the least soluble solid. A similar effect was seen for 10 or 20 wt % $(NH_4)_2SO_4$. However, the least soluble solid is more soluble at 30 wt % $(NH_4)_2SO_4$ for solutions that were 15 or 20 wt % $Na_2C_3H_2O_4$. To determine the identity of the least soluble solid, a single crystal was removed from a 30/20 wt % $(NH_4)_2SO_4$/ $Na_2C_3H_2O_4$ solution at room temperature and analyzed for crystal structure with X-ray crystallography. The analysis determined that the salt present is $NaNH_4SO_4{\cdot}2H_2O$ (sodium ammonium sulfate dihydrate) by a match of the unit cell data with this compound in the Inorganic Crystal Structural Database (ICSD). This is the same compound we found present in the $(NH_4)_2SO_4$/ $NaHC_3H_2O_4/H_2O$ solution, which is not surprising because the same ions are present in solution. Crystals were also removed from this solution and dried for IR analysis. The resulting spectrum showed the characteristic absorption bands for lecontite and showed $Na_2C_3H_2O_4{\cdot}H_2O$ as a minor component (Figure 6).

We then checked other concentrations to determine if there would be an effect on the solids formed; we cooled several solutions of various concentrations in liquid nitrogen until the solution completely solidified. The samples were then placed in an ice bath at 273 K for 30 min. Crystals were removed and allowed to air-dry at room temperature for 24 h. At this point there was no visual sign of liquid, but crystals did appear "wet" by their gray color and crystals would "stick" to a spatula. Samples of the crystals were then placed in an ATR accessory for IR analysis. All of the solutions we made had crystals present at 273 K: 10/15, 10/30, 20/15, 30/10, 30/20 wt % $(NH_4)_2SO_4/Na_2C_3H_2O_4$. For all samples (except the 10/30 wt % $(NH_4)_2SO_4/Na_2C_3H_2O_4$) IR analysis showed the predominant phase to be lecontite crystals. However, there was also indication of solid $Na_2C_3H_2O_4{\cdot}H_2O$ and $Na_2C_3H_2O_4$ in the liquid phase from comparison to our IR spectra for $Na_2C_3H_2O_4$ samples (see Figure 6). In the case of the 10/30 wt % $(NH_4)_2SO_4/Na_2C_3H_2O_4$ sample, IR analysis showed the solid matched the spectrum of $Na_2SO_4$ (Figure 6). This is not a surprising result, because the ratio of $Na^+/NH_4^+$ is quite high, thus favoring formation of $Na_2SO_4$ over lecontite as can be seen in Figure S1 in the Supporting Information. (As noted above, the dry atmospheric conditions of our lab favor the formation of $Na_2SO_4$ over $Na_2SO_4{\cdot}10H_2O$.[38])

We also show the effect of $(NH_4)_2SO_4$ on the glass transition in Figure 7. It is seen that there is a general lowering of $T_g'$ for each concentration of $Na_2C_3H_2O_4$ (5−12 K) independent of the amount of $(NH_4)_2SO_4$ present. In all of the samples we studied, partial crystallization was observed before the glass transition; thus, it is again observed that $T_g'$ is relatively independent of $[Na_2C_3H_2O_4]$.

## DISCUSSION/ATMOSPHERIC IMPLICATIONS

A summary of salt solubilities is given in Figure 8 as a function of mole fraction solute so that solubilities can be compared on a

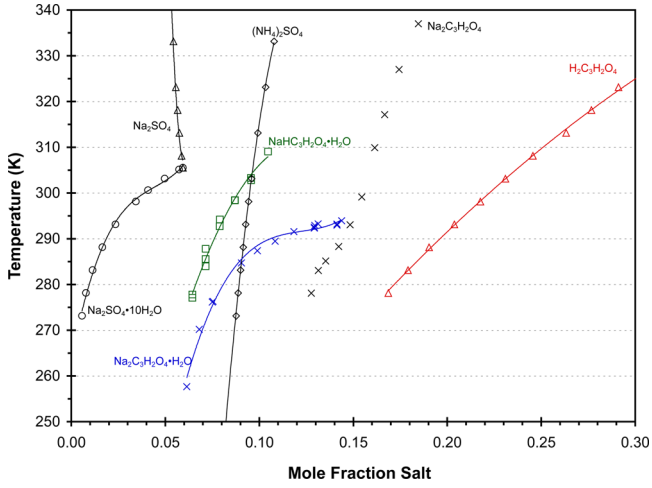


**Figure 8.** Summary of salt solubilities as a function of mole fraction solute. Data for sodium sulfate (black circles and triangles) are from Linke,[37] data for ammonium sulfate (black diamonds) are from Stephen et al.,[34] data for malonic acid (red triangles) are from Hansen and Beyer,[42] and data for $Na_2C_3H_2O_4$ (black crosses) are from Rozaini and Brimblecomb.[39] Data for the sodium malonate hydrates ($Na_2C_3H_2O_4{\cdot}H_2O$, blue crosses; $NaHC_3H_2O_4{\cdot}H_2O$, green squares) are from this study.

mole basis. Malonic acid is the most soluble of the solutes as given in the figure. Sodium malonate monohydrate and sodium hydrogen malonate monohydrate are the next most soluble salts at high temperatures; however, both become less soluble than ammonium sulfate at moderate to low temperatures. This crossing occurs for sodium hydrogen malonate monohydrate at 303 K, and for sodium malonate monohydrate at 285 K. Thus, in the presence of ammonium sulfate, these two organic salts are less soluble than ammonium sulfate at temperatures relevant for the lower and free troposphere. However, as noted above sodium sulfate decahydrate (mirabilite) is even less soluble in these solutions and thus would be expected to precipitate in mixed inorganic/organic aqueous aerosols before the sodium malonates. Under dry conditions or temperatures above 306 K, the decahydrate converts to the anhydrous


DOI: 10.1021/acs.jpca.6b02656
J. Phys. Chem. A 2016, 120, 3827−3834

rhombic form of sodium sulfate (thenardite).[40] Finally, what is not represented in Figure 8 and is the most surprising result is the formation of $NaNH_4SO_4{\cdot}2H_2O$ (lecontite) from mixed ammonium sulfate/sodium malonates solutions. Lecontite is only listed as "soluble" in mineralogy databases (www.mindat.org). This is because the mineral has no actual solubility equilibrium in aqueous solution without other species present. High concentrations of ammonium ions and moderate to high concentrations of sodium and sulfate ions are necessary for lecontite to form from aqueous solution as shown by the $Na_2SO_4/(NH_4)_2SO_4/H_2O$ solubility data (Figure S1 in Supporting Information).[34] Thus, at moderate to low ammonium concentrations in atmospheric aerosols in the presence of sodium and sulfate, we would expect the formation of mirabilite as droplets cool. However, if temperatures remain elevated under dry conditions where aqueous aerosols evaporate, it is possible to move into a concentration region where lecontite is the least soluble substance as we demonstrated in or experiments where crystals were air dried. Additionally, air drying at room temperature was the method used by others to synthesize lecontite in the lab from solutions of equal mole ratio of sodium sulfate and ammonium sulfate with the identity of the crystals confirmed by X-ray crystallography.[35,41] We have illustrated this path to formation of lecontite from low concentrations of sodium and ammonium sulfates in Figure S1 by a dashed line. Another path to lecontite formation in the systems we studied is high ammonium and sulfate concentration at moderate to low sodium concentration. This concentration regime let to lecontite formation at room temperature in solutions that contained either 1:1 or 2:1 sodium:malonate ratios. Thus, even though lecontite does not have a true equilibrium with water, it is a salt that must be considered under dry conditions in atmospheric aerosols where the $Na^+/NH_4^+/SO_4^{2-}$ ratio is 1:1:1 and under high ammonium/sulfate and moderate to high sodium ion concentrations from room temperature and lower with or without the presence of organics.

## SUMMARY

We report here measurements of the solubility of $NaHC_3H_2O_4$ and $Na_2C_3H_2O_4$ in water both with and without $(NH_4)_2SO_4$ present. In both cases, the presence of $(NH_4)_2SO_4$ leads to the precipitation of inorganic compounds such as $Na_2SO_4{\cdot}10H_2O$ (low ammonium content) and $NaNH_4SO_4{\cdot}2H_2O$ (high ammonium content) as the least soluble solids from solution. The latter compound has been known in mineralogy as lecontite but has not previously been recognized as a possible salt component of atmospheric aerosols. After formation of sodium sulfate decahydrate or lecontite, the next least soluble compounds are the sodium malonate hydrates we studied here, $NaHC_3H_2O_4{\cdot}H_2O$ or $Na_2C_3H_2O_4{\cdot}H_2O$. We were able to isolate $Na_2C_3H_2O_4{\cdot}H_2O$ whose crystal structure had not been known, and thus we report for the first time the crystal structure of this salt as determined by X-ray crystallography. Finally, we also report the first infrared spectra of $NaHC_3H_2O_4{\cdot}H_2O$ and $Na_2C_3H_2O_4{\cdot}H_2O$.

We have observed glass transitions in all of the solutions we studied, though partial crystallization of the solution occurred in all $NaHC_3H_2O_4/H_2O$, $NaHC_3H_2O_4/(NH_4)_2SO_4/H_2O$, $Na_2C_3H_2O_4/(NH_4)_2SO_4/H_2O$, and low concentration $Na_2C_3H_2O_4/H_2O$ solutions leading to $T_g'$ values that changed little with malonate salt concentration. However, it was found that the addition of $(NH_4)_2SO_4$ to solutions of either $NaHC_3H_2O_4$ or $Na_2C_3H_2O_4$ had either little or a lowering effect on the value of the glass transition ($T_g'$). For aqueous solutions with $[Na_2C_3H_2O_4] \geq 40$ wt % partial crystallization on cooling was not observed, and thus the entire sample remained liquid up to the glass transition. Hence, the whole sample underwent a true glass transition ($T_g$), which increased with increasing concentration of $Na_2C_3H_2O_4$.

## ASSOCIATED CONTENT

### Supporting Information

The Supporting Information is available free of charge on the ACS Publications website at DOI: 10.1021/acs.jpca.6b02656.

Raw data for the ice melting temperatures, salt solubilities, and glass transitions for the systems studied in this paper are found in the following tables: Table S1, $NaHC_3H_2O_4/H_2O$; Table S2, $(NH_4)_2SO_4/NaHC_3H_2O_4/H_2O$; Table S3, $Na_2C_3H_2O_4/H_2O$; Table S4, $(NH_4)_2SO_4/Na_2C_3H_2O_4/H_2O$. A plot of the $Na_2SO_4/(NH_4)_2SO_4/H_2O$ solubility data from Stephen et al.[34] is given in Figure S1. Details are given regarding the structural solution and refinement for $Na_2C_3H_2O_4{\cdot}H_2O$ with Figures S2−S4 showing further molecular drawings of the structure. Tables S5−S12 give the crystal structure parameters. (PDF)

Crystallographic information. (CIF)

## AUTHOR INFORMATION

### Corresponding Author

*E-mail: kbeyer@uwalx.edu. Phone: 608-785-8292.

### Notes

The authors declare no competing financial interest.

## ACKNOWLEDGMENTS

This work was supported by the NSF Atmospheric Chemistry Program (AGS-1361592).

## REFERENCES

(1) Murphy, D. M.; Thomson, D. S.; Mahoney, T. M. J. In Situ Measurements of Organics, Meteoritic Material, Mercury, and Other Elements in Aerosols at 5 to 19 Kilometers. *Science* **1998**, *282*, 1664−1669.

(2) Froyd, K. D.; Murphy, D. M.; Lawson, P.; Baumgardner, D.; Herman, R. L. Aerosols That Form Subvisible Cirrus at the Tropical Tropopause. *Atmos. Chem. Phys.* **2010**, *10* (1), 209−218.

(3) Sullivan, R. C.; Prather, K. A. Investigations of the Diurnal Cycle and Mixing State of Oxalic Acid in Individual Particles in Asian Aerosol Outflow. *Environ. Sci. Technol.* **2007**, *41* (23), 8062−8069.

(4) Seinfeld, J. H.; Pandis, S. N. *Atmospheric Chemistry and Physics: From Air Pollution to Climate Change*; Wiley: New York, 1998.

(5) Harris, E.; Sinha, B.; Foley, S.; Crowley, J. N.; Borrmann, S.; Hoppe, P. Sulfur Isotope Fractionation during Heterogeneous Oxidation of SO2 on Mineral Dust. *Atmos. Chem. Phys.* **2012**, *12* (11), 4867−4884.

(6) Reitz, P.; Spindler, C.; Mentel, T. F.; Poulain, L.; Wex, H.; Mildenberger, K.; Niedermeier, D.; Hartmann, S.; Clauss, T.; Stratmann, F.; et al. Surface Modification of Mineral Dust Particles by Sulphuric Acid Processing: Implications for Ice Nucleation Abilities. *Atmos. Chem. Phys.* **2011**, *11* (15), 7839−7858.

(7) Harris, E.; Sinha, B.; van Pinxteren, D.; Tilgner, A.; Fomba, K. W.; Schneider, J.; Roth, A.; Gnauk, T.; Fahlbusch, B.; Mertes, S.; et al. Enhanced Role of Transition Metal Ion Catalysis During In-Cloud Oxidation of SO2. *Science* **2013**, *340* (6133), 727−730.



DOI: 10.1021/acs.jpca.6b02656
J. Phys. Chem. A 2016, 120, 3827−3834

(8) Kerminen, V.-M.; Teinilä, K.; Hillamo, R.; Pakkanen, T. Substitution of Chloride in Sea-Salt Particles by Inorganic and Organic Anions. *J. Aerosol Sci.* **1998**, *29* (8), 929−942.
(9) Kojima, T.; Buseck, P. R.; Iwasaka, Y.; Matsuki, A.; Trochkine, D. Sulfate-Coated Dust Particles in the Free Troposphere over Japan. *Atmos. Res.* **2006**, *82* (3−4), 698−708.
(10) Laskin, A.; Moffet, R. C.; Gilles, M. K.; Fast, J. D.; Zaveri, R. A.; Wang, B.; Nigge, P.; Shutthanandan, J. Tropospheric Chemistry of Internally Mixed Sea Salt and Organic Particles: Surprising Reactivity of NaCl with Weak Organic Acids. *J. Geophys. Res.* **2012**, *117* (D15), D15302.
(11) Reid, J. S.; Koppmann, R.; Eck, T. F.; Eleuterio, D. P. A Review of Biomass Burning Emissions Part II: Intensive Physical Properties of Biomass Burning Particles. *Atmos. Chem. Phys.* **2005**, *5* (3), 799−825.
(12) Zauscher, M. D.; Wang, Y.; Moore, M. J. K.; Gaston, C. J.; Prather, K. A. Air Quality Impact and Physicochemical Aging of Biomass Burning Aerosols during the 2007 San Diego Wildfires. *Environ. Sci. Technol.* **2013**, *47* (14), 7633−7643.
(13) Hinz, K.-P.; Trimborn, A.; Weingartner, E.; Henning, S.; Baltensperger, U.; Spengler, B. Aerosol Single Particle Composition at the Jungfraujoch. *J. Aerosol Sci.* **2005**, *36* (1), 123−145.
(14) Murphy, D. M.; Cziczo, D. J.; Froyd, K. D.; Hudson, P. K.; Matthew, B. M.; Middlebrook, A. M.; Peltier, R. E.; Sullivan, A.; Thomson, D. S.; Weber, R. J. Single-Particle Mass Spectrometry of Tropospheric Aerosol Particles. *J. Geophys. Res. Atmospheres* **2006**, *111*, D23S32.
(15) Sullivan, R. C.; Guazzotti, S. A.; Sodeman, D. A.; Prather, K. A. Direct Observations of the Atmospheric Processing of Asian Mineral Dust. *Atmos. Chem. Phys.* **2007**, *7* (5), 1213−1236.
(16) Cziczo, D. J.; Froyd, K. D.; Hoose, C.; Jensen, E. J.; Diao, M.; Zondlo, M. A.; Smith, J. B.; Twohy, C. H.; Murphy, D. M. Clarifying the Dominant Sources and Mechanisms of Cirrus Cloud Formation. *Science* **2013**, *340* (6138), 1320−1324.
(17) Ghorai, S.; Wang, B.; Tivanski, A.; Laskin, A. Hygroscopic Properties of Internally Mixed Particles Composed of NaCl and Water-Soluble Organic Acids. *Environ. Sci. Technol.* **2014**, *48* (4), 2234−2241.
(18) Wang, B.; O'Brien, R. E.; Kelly, S. T.; Shilling, J. E.; Moffet, R. C.; Gilles, M. K.; Laskin, A. Reactivity of Liquid and Semisolid Secondary Organic Carbon with Chloride and Nitrate in Atmospheric Aerosols. *J. Phys. Chem. A* **2015**, *119* (19), 4498−4508.
(19) Clegg, S. L.; Seinfeld, J. H. Thermodynamic Models of Aqueous Solutions Containing Inorganic Electrolytes and Dicarboxylic Acids at 298.15 K. 1. The Acids as Nondissociating Components. *J. Phys. Chem. A* **2006**, *110*, 5692−5717.
(20) Clegg, S. L.; Seinfeld, J. H. Thermodynamic Models of Aqueous Solutions Containing Inorganic Electrolytes and Dicarboxylic Acids at 298.15 K. 2. Systems Including Dissociation Equilibria. *J. Phys. Chem. A* **2006**, *110*, 5718−5734.
(21) Zobrist, B.; Marcolli, C.; Pedernera, D. A.; Koop, T. Do Atmospheric Aerosols Form Glasses? *Atmos. Chem. Phys.* **2008**, *8* (17), 5221−5244.
(22) Koop, T.; Bookhold, J.; Shiraiwa, M.; Pöschl, U. Glass Transition and Phase State of Organic Compounds: Dependency on Molecular Properties and Implications for Secondary Organic Aerosols in the Atmosphere. *Phys. Chem. Chem. Phys.* **2011**, *13* (43), 19238−19255.
(23) Murray, B. J.; Wilson, T. W.; Dobbie, S.; Cui, Z.; Al-Jumur, S. M. R. K.; Möhler, O.; Schnaiter, M.; Wagner, R.; Benz, S.; Niemand, M.; et al. Heterogeneous Nucleation of Ice Particles on Glassy Aerosols under Cirrus Conditions. *Nat. Geosci.* **2010**, *3* (4), 233−237.
(24) Schubnell, M. Temperature and Heat Flow Calibration of a DSC-Instrument in the Temperature Range Between-100 and 160 Degrees C. *J. Therm. Anal. Calorim.* **2000**, *61*, 91−98.
(25) Zhang, R.; Wooldridge, P. J.; Abbatt, J. P. D.; Molina, M. J. Physical-Chemistry of the H2SO4/H2O Binary-System at Low-Temperatures - Stratospheric Implications. *J. Phys. Chem.* **1993**, *97*, 7351−7358.
(26) Lide, D. R. *Handbook of Chemistry and Physics*; CRC Press: Boca Ratan, 1993.
(27) Power, S.; Hughs, D. S.; Hursthouse, M. B.; Threlfall, T. L. Private Communication, 2014.
(28) Angell, C. A. Liquid Fragility and the Glass Transition in Water and Aqueous Solutions. *Chem. Rev.* **2002**, *102* (8), 2627−2650.
(29) Dette, H. P.; Koop, T. Glass Formation Processes in Mixed Inorganic/Organic Aerosol Particles. *J. Phys. Chem. A* **2015**, *119* (19), 4552−4561.
(30) Roos, Y.; Karel, M. Amorphous State and Delayed Ice Formation in Sucrose Solutions. *Int. J. Food Sci. Technol.* **1991**, *26* (6), 553−566.
(31) Roos, Y. H. Glass Transition Temperature and Its Relevance in Food Processing. *Annu. Rev. Food Sci. Technol.* **2010**, *1* (1), 469−496.
(32) Arzt, S.; Glazer, A. M. The Optical Activity and Absolute Optical Chirality of $NaNH_4SO_4{\cdot}2H_2O$. *Acta Crystallogr., Sect. B: Struct. Sci.* **1994**, *50* (4), 425−431.
(33) Faust, R. J.; Bloss, F. D. X-Ray Study of Lecontite. *Am. Mineral.* **1963**, *48*, 180−188.
(34) Stephen, H.; Stephen, T.; Silcock, H. L. *Solubilities of Inorganic and Organic Compounds*; Macmillan: New York, 1963.
(35) Kloprogge, J. T.; Broekmans, M.; Duong, L. V.; Martens, W. N.; Hickey, L.; Frost, R. L. Low Temperature Synthesis and Characterisation of Lecontite, $(NH_4)Na(SO_4){\cdot}2H_2O$. *J. Mater. Sci.* **2006**, *41*, 3535−3539.
(36) NIST Standard Reference Database 69. *NIST Chemistry WebBook*, (accessed January 25, 2016).
(37) Linke, W. F. *Solubilities: Inorganic and Metal Organic Compounds: A Revision and Continuation of the Compilation by A. Seidell*, 4th ed.; Van Nostrand: New York, 1958; (2 volumes).
(38) Linnow, K.; Zeunert, A.; Steiger, M. Investigation of Sodium Sulfate Phase Transitions in a Porous Material Using Humidity- and Temperature-Controlled X-Ray Diffraction. *Anal. Chem.* **2006**, *78* (13), 4683−4689.
(39) Rozaini, M. Z. H.; Brimblecombe, P. The Solubility Measurements of Sodium Dicarboxylate Salts; Sodium Oxalate, Malonate, Succinate, Glutarate, and Adipate in Water from T = (279.15 to 358.15) K. *J. Chem. Thermodyn.* **2009**, *41* (9), 980−983.
(40) Steiger, M.; Asmussen, S. Crystallization of Sodium Sulfate Phases in Porous Materials: The Phase Diagram Na2SO4-H2O and the Generation of Stress. *Geochim. Cosmochim. Acta* **2008**, *72*, 4291−4306.
(41) Corazza, E.; Sabelli, C. The Crystal Structure of Lecontite, $NaNH_4SO_4{\cdot}2H_2O$. *Acta Crystallogr.* **1967**, *22* (5), 683−687.
(42) Hansen, A. R.; Beyer, K. D. Experimentally Determined Thermochemical Properties of the Malonic Acid/water System: Implications for Atmospheric Aerosols. *J. Phys. Chem. A* **2004**, *108*, 3457−3466.


DOI: 10.1021/acs.jpca.6b02656
*J. Phys. Chem. A* 2016, 120, 3827−3834